Classification Techniques For Autistic vs. Typically Developing Brain Using MRI Data

Rachid Fahmi, et al.

IEEE, 2007

NeuroSpectrum Insights, Inc.
info@neurospectruminsights.com
www.neurospectruminsights.com

CLASSIFICATION TECHNIQUES FOR AUTISTIC VS. TYPICALLY DEVELOPING BRAIN USING *MRI* DATA

Rachid Fahmi[1] *, Ayman S. El-Baz* [2]*, Hossam E Abd El Munim*[1]*, Aly A. Farag*[1]*, and Manuel F. Casanova*[3]

[1]Computer Vision and Image Processing Laboratory (*CVIP* Lab.), University of Louisville
[2]Bioengineering Department, University of Louisville
[3] Department of Psychiatry and Behavioral Sciences , University of Louisville

ABSTRACT

Autism is a neurodevelopmental disorder that disrupts social and cognitive functions. Various autism studies revealed abnormalities in several brain regions. There is an increasing agreement from structural imaging studies on the abnormal anatomy of the white matter (*WM*) in autistic brains. In addition, the deficits in the size of the corpus callosum (*CC*) and its sub-regions in patients with autism relative to controls are well established. This paper presents two novel classification techniques of autism based on structural *MRI*. Our analysis is based on shape descriptions and geometric models. We compute the 3D distance map to describe the shape of the *WM* and use it as a statistical feature to discriminate between the two groups. We also use our recently proposed non-rigid registration technique [1] to devise another classification approach by statistically analyzing and comparing the deformation fields generated from registering *CC*'s onto each others. The accuracy of our techniques was tested on postmortem and on in-vivo brain MR data. The results are very promising and show that, contrary to traditional methods, the proposed techniques are less sensitive to age and volume effects.

1. INTRODUCTION

Autism is a neurodevelopmental disorder characterized by impairments in social interaction, communications, and the presence of unusual behaviors and interests. Autism is a spectrum disorder that typically appears during the first three years of life and last throughout a person's life with a wide range of severity. Autism makes no racial, ethnic, or socioeconomic distinctions, and is four times more likely to occur in boys than girls. According to the Centers for Disease Control and Prevention (C.D.C.), about 1 in 150 American children fall somewhere in the autistic spectrum. There is no cure for autism; however, therapies targeting specific symptoms may result in substantial improvement, particularly when started at a young age.

This work is supported by the University of Louisville Department of Psychiatry and the CVIP lab. Corresponding author: Aly Farag– farag@cairo.spd.louisville.edu .

Neuroimaging and neuropathological studies have revealed a great deal concerning the pathogenesis of autism. Most of these studies have reported increased brain weight and volume (*macroencephaly*) in autistic patients [2, 3]. Interestingly, *MRI* studies have shown an increased volume in cerebellar white matter (*WM*) of young children with autism relative to controls, while no difference was found in the cerebellar gray matter (*GM*) volume except in older patients [4]. Cortical *GM* enlargement, particularly in the frontal and temporal lobes, is another abnormal feature of the brain of autistic patients [5]. In addition, a number of imaging studies reported that the *CC* has reduced size in autistic subjects (e.g., [6, 7]); however, findings are inconsistent as to which segment of the *CC* is abnormal. Some of these studies have reported reduction in the size of the body and the posterior sub-regions of the *CC* in autistic patients [8], whereas other studies have found that the reduction was limited to the body and the anterior segment of the *CC* [9]. Recently, computational mapping methods were used in an *MRI* study by Vidal et al. [10] to investigate *CC* abnormalities in male patients with autism. This study revealed significant reductions in both the splenium and genu of the *CC* in autistic sufferers relative to controls.

As an attempt to explain the pervasive symptomatology of autism, it is theorized that the increase in brain volume measured in the autistic brain is mainly due to an abnormally large *WM* volume [11]. Casanova et al. [12] attribute this abnormality to the increased number of minicolumns (*the basic functional unit of the brain that organizes neurons in cortical space* [13, 12]) in autism. This increase in the total number of minicolumns in autism requires a scale increase (roughly a $3/2$ power law) in *WM* to maintain modular interconnectivity [14]. Anatomically these results can be seen in structural *MRI* studies as an increase in the outer radiate compartment of *WM* [11]. These findings, compared to the reported deficits of the size of the *CC*, explain why autistics excel in performance in tasks that require information processing within a given brain area (e.g., visual discrimination) but otherwise perform poorly in those that require inter-areal integration (e.g., joint attention, language).

Recently, we have implemented an algorithm that measures

the gyrification window and used it to derive a macroscopic neuropathological correlate to autism which relates to neuronal connectivity [15]. The presented study offers a new approach to the classification of autism based on structural *MRI*, and may provide for a biomarker in autism that allows for construct validity among varied studies.

In this work, we aim at using the reported abnormalities in the *WM* and the *CC* in order to devise new classification methods of autism through *MRI* analyzes. To overcome the limitations and shortcomings of the volumetric studies, we base our analyzes on shape descriptions and geometric models. We compute the 3D distance map as a shape descriptor of the *WM*. The distribution of this distance map is then used as a statistical feature that allows the discrimination between the two groups. We also use our non-rigid registration technique [1] to devise a new classification approach by analyzing the deformation fields generated from 3D registration of *CC*'s onto each others. Results on both post-mortem and in-vivo *MRI*s are presented to show the potential of the proposed classification techniques.

2. METHODS AND MATERIALS

2.1. Subjects and Image Acquisitions

Two types of *MR* brain data are used in this study: postmortem proton density (*P.D.*)-weighted *MRI* data, and in-vivo T1-weighted *MRI* data. The latter will be referred to as the Savant Data in this paper.

The description of the postmortem *MRI* data used in this study is presented in detail in [16]. Postmortem brains from 23 autistic patients (mean interval between death and autopsy: 25.8 hrs) and from 16 controls (mean interval between death and autopsy: 20.4 hrs) are considered. Due to the imaging procedure [16], geometric distortions such as large deep cuts, commonly occur and are revealed in the *MRI* scans (see Fig. 1). The Savant data sets were acquired with the same 1.5 T Signa *MRI* scanner. A total of 30 normals and 15 autistic brain data sets were collected. Each data set is of size $256 \times 256 \times 124$ and a slice resolution of $0.9375 \times 0.9375 \times 1.5 mm^3$.

2.2. Image Processing and Analysis

The data at hand undergo a series of preprocessing steps. First, all data sets are smoothed using the anisotropic diffusion filter. Then the publicly available brain extraction algorithm (*BET2/FSL*) is applied to get rid of the non-brain tissues in the Savant images.

Image Segmentation: We use our level set based-adaptive multi modal image segmentation approach [17] to segment the images into *WM*, GM, and CSF. This method builds a statistical Gaussian model with adaptive parameters for each region to be segmented. These models are explicitly embedded into the *PDE*s governing the curves evolution. The parameters of each region are initially estimated using the Stochastic *EM* algorithm and are automatically re-estimated at each iteration. Fig. 1 shows some results of our segmentation technique when applied to some T1-weighted *MRI* scans to extract the *WM*, GM, and CSF.

Distance Map and Shape Description: Distance map, $D(\mathbf{x})$, assigns to each point in a given image a minimal distance from a locus of points (usually object boundaries). The exact computation of $D(\mathbf{x})$ is very time consuming, especially for large data sets. In this work, we approximate $D(\mathbf{x})$ using the Multi-Stencils Fast Marching (MSFM) method [18].

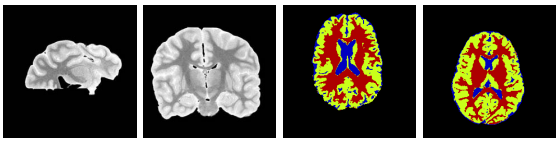

Fig. 1. Left 2 columns: Samples of postmortem data. Right: Segmentation results on Savant data.

Non-Rigid Image Registration: We recently present a novel and accurate approach for nonrigid registration [1]. New feature descriptors are built as voxel signatures using scale space theory. These descriptors are used to capture the global motion of the imaged object. Local deformations are modeled through an evolution process of equi-spaced closed curves/surfaces (iso-contours/-surfaces) which are generated using fast marching level sets and are matched using the built feature descriptors.

3. PROPOSED CLASSIFICATION APPROACHES

The main objective of this study is to exploit the reported anomalies of the *WM* and the *CC* in autistic sufferers in order to devise new *MRI*-based classification methods of autism. Our approaches are based on shape descriptions and geometrical models, and are then less sensitive to age and the effect of other confounding factors compared to volumetric-based methods.

3.1. White Matter Shape Analysis

Both postmortem and savant data are used in this analysis. Note that the *WM* was segmented using our level set based segmentation technique as explained in Sec. 2.2.

Our first classification technique is derived as follows. First, we randomly select a sample set for each group (16 controls and four autistic from the savant data; and six controls and four autistics from the postmortem data), and we compute the distance maps inside of their segmented *WM*'s. Then, we compute their corresponding Cumulative Distribution Functions (*CDF*). Furthermore, in order to remove the volume effect, these *CDF*s are normalized between 0 and 1 before being averaged as shown on Fig. 2.

Finally, given an unknown subject to be classified, we first compute and normalize the *CDF* of the distance map inside

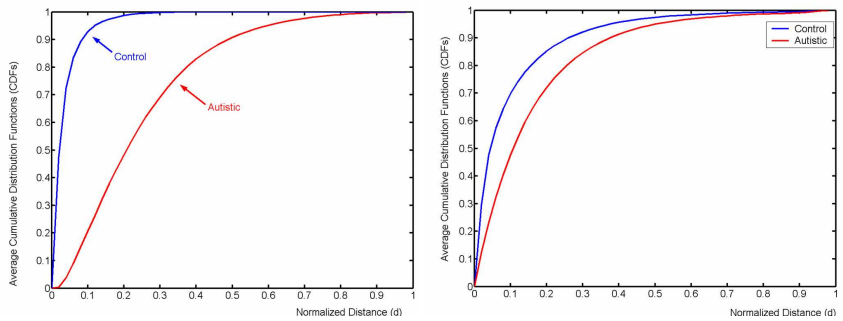

Fig. 2. Average normalized *CDF*s of the distance map inside the *WM* of 4 autistic and 16 controls from savant data (left); and of 4 autistic and 6 controls from postmortem data (right). Note the clear discrimination of the two classes when using the distribution of the distance map inside the *WM*.

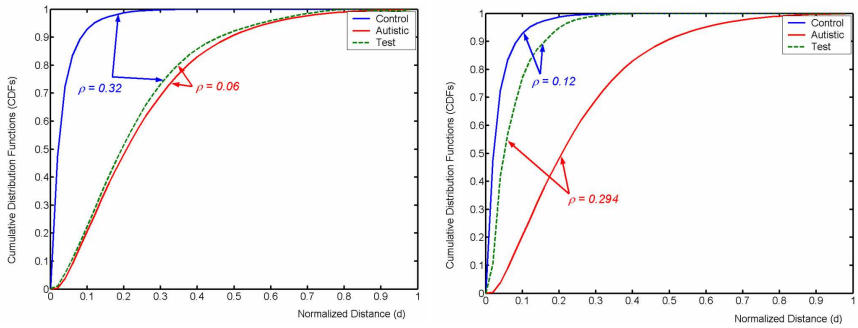

Fig. 3. Classification of unknown (dotted) using the Lévy distance ρ. Left: the unknown subject (dotted) is classified as control. Right: another test subject is classified as autistic.

of its segmented *WM*. This *CDF* is then compared to the two average *CDF*'s (autistic and control) using the Lévy distance. The smallest Lévy distance indicates the class to which the test subject belongs. Figure 3 shows the classification results of two test subjects from the savant data sets. Both subjects were classified successfully.Table 1 summarizes the performance of the proposed classification method on each type of data.

Table 1. Performance of the *WM*-based classification approach.

Confidence Rate	Autistic		Control	
	P-mortem	Savant	P-mortem	Savant
85%	14/14	13/15	12/12	30/30
90%	13/14	12/15	12/12	30/30
95%	13/14	11/15	11/12	28/30

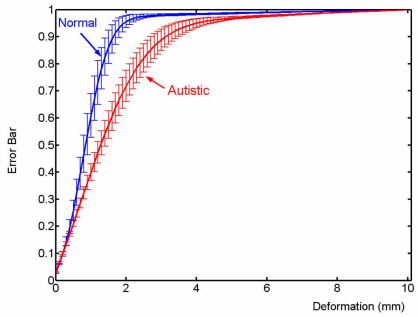

Fig. 4. Error Bar. The curves represent the average *CDF*s of displacement fields resulting from the registration of 3 subjects to the reference within each group from the savant data.

3.2. Corpus callosum analysis

The main goal is to use the difference in the *CC* anatomy in order to devise a classification technique between the two groups. Unlike the traditional approaches, which are sensitive to the segmentation outputs as well to the effect of volume, we propose a novel classification approach based on analyzing the displacement fields generated from the non-rigid registration of different *CC*s onto a chosen reference within each group. Due to the distortions in the postmortem images, which made the segmentation of the *CC* from these images very challenging, only the savant data sets are used in this analysis. For this data, the *CC*s are extracted manually from the segmented brain images.

For each group, we randomly picked four *CC* data sets, one of which is chosen as reference and the remaining ones are

registered to it using our deformable registration method [1]. Three Deformation Fields (*DF*'s) are then generated and averaged for each group. A *CDF* is computed to represent the changes of the magnitudes of each one of these two averaged deformation fields as shown in Fig. 4.
Given an unknown subject, we register it, one at a time to the chosen control reference and then to the chosen autistic reference. Two *DF*s are then generated, and their *CDF*s are computed. These *CDF*s are finally compared to the "average" *CDF*s representing each class using the Lévy distance. The smallest of the resulting distances indicates indicates the class to which the tested subject belongs. Table 2 summarizes the classification performances for each group.

Table 2. Performance of the *CC*-based classification.

Confidence Rate	Autistic		Control	
	P-mortem	Savant	P-mortem	Savant
85%	-	10/15	-	29/30
90%	-	9/15	-	29/30
95%	-	7/15	-	25/30

4. CONCLUSION

In this work, we have presented two new neuroimaging based classification techniques that allow the discrimination between autistic and typically developing brains. These approaches are motivated by the reported abnormal anatomy of the *WM* and the *CC* in autistic sufferers. Statistical features were carefully extracted from the *MRI*s and served to discriminate between the two groups. We tested our approaches on post-mortem as well as on in-vivo brain *MRI*s with different modalities. The proposed methods result in significant accuracy as summarized in tables 1 and 2. Contrary to the methods that emphasize volumetric measures, our methods are based on geometrical models and shape analysis, and hence showed no sensitivity to age variations. Different brain structures will be investigated in future works, and other images modalities (e.g., *fMRI*s, *DTI*s, etc) will be considered to enhance the output of our techniques.

5. REFERENCES

[1] R. Fahmi, A. Abdel-Hakim Aly, A. El-Baz, and A. Farag, "New deformable registration technique using scale space and curve evolution theory and a finite element based validation framework.," in *IEEE EMBS'06*, New York, NY, Aug-Sep 2006, pp. 3041–3044.

[2] L. Kanner, "Autistic disturbances of affective contact.," *Nervous Child*, vol. 2, pp. 250–250, 1943.

[3] R. Courchesne, R. Carper, and N. Akshoomoff, "Evidence of brain overgrowth in the first year of life in autism.," *JAMA*, vol. 290, pp. 337–344, 2003.

[4] E. Courchesne et al., "Unusual brain growth patterns in early life in patients with autistic disorder: an mri study.," *Neurology*, vol. 57, no. 2, pp. 245–254, 2001.

[5] R.A. Carper, P. Moses, Z.D. Tigue, and E. Courchesne, "Cerebral lobes in autism: early hyperplasia and abnormal age effects.," *Neuroimage*, vol. 16, pp. 1038–1051, 2002.

[6] A.Y. Hardan, N.J. Minshew, and M.S. Keshavan, "Corpus callosum size in autism.," *Neurology*, vol. 55, pp. 1033–1036, 2000.

[7] N .Barnea-Goraly, H. Kwon, V. Menon, S. Eliez, L. Lotspeich, and A.L. Reiss, "White matter structure in autism: Preliminary evidence from diffusion tensor imaging.," *Biol. Psychiatry*, vol. 55, pp. 323–326, 2004.

[8] J. Piven, J. Bailey, B.J. Ranson, and S. Arndt, "An mri study of the corpus callosum in autism.," *Am. J. Psychiatry*, vol. 154, no. 8, pp. 1051–1056, 1997.

[9] F. Manes, J. Piven, D. Vrancic, V. Nanclares, C. Plebst, and S. Starkstein, "An MRI study of the corpus callosum and cerebellum in mentally retarded autistic individuals.," *J. Neuropsychiatry Clin Neurosci.*, vol. 11, pp. 470–474, 1999.

[10] C.N. Vidal, R. Nicolson, T.J. DeVito, K.M. Hayashi, J.A. Geaga, D.J. Drost, P.C. Williamson, N. Rajakumar, Y .Sui, R.A. Dutton, A.W. Toga, and P.M. Thompson, "Mapping corpus callosum deficits in autism: An index of aberrant cortical connectivity.," *Biol Psychiatry.*, vol. 60, no. 3, pp. 218–225, 2006.

[11] M.R. Herbert, D.A. Ziegler, N. Makris, P.A. Filipek, T.L. Kemper, J.J. Normandin, H.A.Sanders, D.N. Kennedy, and V.S. Jr Caviness, "Localization of white matter volume increase in autism and developmental language disorder.," *Ann. Neurol.*, vol. 55, pp. 530–540, 2004.

[12] M. F. Casanova, I.A. van Kooten, A. Switala, H. van Engeland, H. Heinsen, H. Steinbusch, P. R. Hof, J. Trippe, J. Stone, and C. Schmitz, "Minicolumnar abnormalities in autism.," *Acta Neuropathological. In press (Available Online).*, 2006.

[13] V. B. Mountcastle, "Introduction. computation in cortical columns.," *Cereb. Cortex*, vol. 13, no. 1, pp. 2–4, 2003.

[14] M. F. Casanova, "White matter volume increases and minicolumns in autism.," *Ann. Neurol.*, vol. 56, pp. 453–, 2004.

[15] M. F. Casanova, A. Farag, A. El-Baz, M. Mott, H. Hassan, R. Fahmi, and A. E. Switala, "Abnormalities of the gyral window in autism: a macroscopic correlate to a putative minicolumnopathy.," *J. of special education and rehabilitation*, vol. 1-2, pp. 85–101, 2007.

[16] C.M. Schumann, H.M. Buonocore, and D.G. Amaral, "Magnetic resonance imaging of the post-mortem autistic brain," *J. of Autism and Developmental Disorders*, vol. 31, no. 6, pp. 561–568, 2001.

[17] Aly A. Farag and Hossam Hassan, "Adaptive segmentation of multi-modal 3d data using robust level set techniques.," in *Proc. of MICCAI'04*, Saint-Malo, France, September 26-29 2004, pp. 143–150.

[18] M. Sabry Hassouna and A. A. Farag, "Accurate tracking of monotonically advancing fronts," in *Proc. CVPR'06*, New York, NY, June 2006, pp. 355–362.